# Nanocomposite Polymer Electrolytes Containing Silica Nanoparticles: Comparison Between Poly(ethylene glycol) and Poly(ethylene oxide) Dimethyl Ether

**Jung Tae Park,[1] Kyung Ju Lee,[1] Moon-Sung Kang,[2] Yong Soo Kang,[3] Jong Hak Kim[1]**

[1]*Department of Chemical Engineering, Yonsei University, Seodaemun-Gu, Seoul 120-749, South Korea*
[2]*Energy Laboratory, Corporate R&D Center, Samsung SDI Co., Giheung-Gu, Yongin-Si, Gyeonggi-Do 449-577, South Korea*
[3]*Department of Chemical Engineering, Hanyang University, Seongdong-Gu, Seoul 133-791, South Korea*

Received 4 February 2007; accepted 9 May 2007
DOI 10.1002/app.26951
Published online 5 September 2007 in Wiley InterScience (www.interscience.wiley.com).

**ABSTRACT:** Nanocomposite polymer electrolytes consisting of low molecular weight poly(ethylene oxide) (PEO), iodine salt MI (M = $K^+$, imidazolium$^+$), and fumed silica nanoparticles have been prepared and characterized. The effect of terminal group in PEO, i.e., hydroxyl (—OH) and methyl ($CH_3$) using poly(ethylene glycol) (PEG) and PEO dimethyl ether (PEODME), respectively, was investigated on the interactions, structures, and ionic conductivities of polymer electrolytes. Wide angle X-ray scattering (WAXS), differential scanning calorimetry (DSC), and complex viscosity measurements clearly showed that the gelation of PEG electrolytes occurred more effectively than that of PEODME electrolytes. It was attributed to the fact that the hydroxyl groups of PEG participated in the hydrogen-bonding interaction between silica nanoparticles, and consequently helped to accelerate the gelation reaction, as confirmed by FTIR spectroscopy. Because of its interaction, the ionic conductivities of PEG electrolytes (maximum value $\sim 6.9 \times 10^{-4}$ S/cm) were lower than that of PEODME electrolytes ($2.3 \times 10^{-3}$ S/cm). © 2007 Wiley Periodicals, Inc. J Appl Polym Sci 106: 4083–4090, 2007

**Key words:** nanocomposite; polymer electrolyte; conductivity; spectroscopy; gelation; nanoparticles

## INTRODUCTION

The term ''polymer electrolyte'' may refer to a material, which comprises metal salts dissolved in a polymeric matrix or the polymer backbones with covalently bonded ionizing groups attached to them.[1–4] The latter ''polymer electrolyte'' is sometimes called ''polyelectrolyte'' and essentially has a proton conducting property to be used as the electrolyte in proton exchange membrane fuel cells (PEMFC).[5,6] The former ''polymer electrolyte'' commonly contains polar moieties such as ether, ester, or amide linkages in a polymer matrix to dissolve metal salts effectively. Thus, the dissolving behavior and ionic constituents of metal salts in the polymer matrix are very important in determining physical properties, particularly the ionic conduction and mass transport properties.[7,8] These properties of polymer electrolytes have been used in the area of lithium polymer batteries,[9,10] dye-sensitized solar cells (DSSCs),[11–13] and separation membranes.[14,15]

Recently, polymer electrolytes containing inorganic nanoparticles have received great attention due to their superior transport properties.[16–18] Ionic conductivities were significantly enhanced by adding nanoparticles 10 wt % to poly(ethylene oxide) (PEO)/$LiClO_4$ electrolytes.[19] In addition, inorganic nanoparticles such as $TiO_2$ and $ZrO_2$ have been used to increase the conductivity of polyaniline nanocomposites.[20,21] Ceramic fillers also appeared to enhance the mechanical properties of PEO polymer electrolytes at temperatures above the melting point of PEO.[22] The conductivity enhancement by nanosized $SnO_2$ fillers in the hybrid polymer electrolyte PEO–$SnO_2$–$LiClO_4$ has been elucidated by the fact that the oxygen vacancies on $SnO_2$ surface were regarded as the active Lewis acidic sites that interact with both PEO segments and $ClO_4^-$ ions leading to conductivity improvement.[23] The NMR results also demonstrated that the increased ionic conductivity is not attributed to a corresponding increase in polymer segmental motion, but more likely a weakening of the polyether-cation association induced by the nanoparticles.[24] Our group also have demonstrated that the introduction of fumed silica nanoparticles into PEO matrix produced the improved DSSC performance and excellent mechanical properties.[12] Hydroxyl groups attached to the surface of fumed

*Correspondence to:* J. H. Kim (jonghak@yonsei.ac.kr).
Contract grant sponsor: Ministry of Education (the second stage Brain Korea 21 Program at Yonsei University).

silica nanoparticles make the surface hydrophilic and capable of hydrogen bonding. With these properties, fumed silica nanoparticles create a three-dimensional network that prevents the viscous flow of low molecular weight polymer, and thus providing the required mechanical strength of polymer electrolytes.[25–27]

In this study, the composite polymer electrolytes consisting of low molecular weight PEO, iodine salt MI (M = $K^+$, imidazolium$^+$), and fumed silica nanoparticles have been prepared and characterized. Especially two kinds of electrolyte medium, i.e., poly (ethylene glycol) (PEG) and PEO dimethyl ether (PEODME), were compared to investigate the effect of terminal group in PEO, i.e., hydroxyl (—OH) and methyl ($CH_3$). The coordinative interaction and structural changes in the polymer electrolytes were characterized using FTIR spectroscopy, wide angle X-ray scattering (WAXS), differential scanning calorimetry (DSC), and complex melt viscosity.

## EXPERIMENTAL

PEG ($M_n$ = 400 g/mol), PEOME ($M_n$ = 500 g/mol), potassium iodide (KI, 99.998%), and fumed silica nanoparticles were purchased from Aldrich Chemical. Fumed silica nanoparticles have a diameter of 11 nm, surface area of 255 ± 15 $m^2/g$, density of 4.5 ± 0.5 $lb/ft^3$, and 3.5–4.5 OH groups/$\mu m^2$. Fumed silica nanoparticles are also amorphous, as determined from XRD. Especially, —OH become attached to some of Si atoms on the surface of particles, making the surface hydrophilic and capable of hydrogen bonding with suitable molecules. Thus, silica nanoparticles aggregate to form a network structure at higher silica concentration, mostly due to hydrogen-bonding interaction.

1-Methyl-3-propylimidazolium iodide (MPII) was purchased from Solaronix, Switzerland. All chemicals were used without further purification. Predetermined amounts of polymer and iodine salt were dissolved in acetonitrile (99.8%, anhydrous) together. The mole ratio of ether oxygen of polymer to iodide salt was always fixed at 20. Different amounts of fumed silica nanoparticles were added to the polymer solutions. The solutions were cast on a Teflon-glass plate and dried in a dry $N_2$ environment to minimize the presence of water in the film. The films were further dried in a vacuum oven for 2 days at 40°C.

FTIR measurements were performed on a 6030 Mattson Galaxy Series FTIR spectrometer; 128–128 scans were signal-averaged at a resolution of 2 $cm^{-1}$. WAXS was utilized with Cu Kα radiation to characterize the structure of polymer electrolytes at a scanning speed of 5°/min. Differential scanning calorimeter (DSC 2920, TA Instruments) was used to measure glass transition temperature ($T_g$) of the polymer electrolytes at a heating rate of 10°C/min under $N_2$ environment. Complex melt viscosities of the materials were determined at room temperature using disk-plate shape rheometer (RheoStress1, HAAKE).

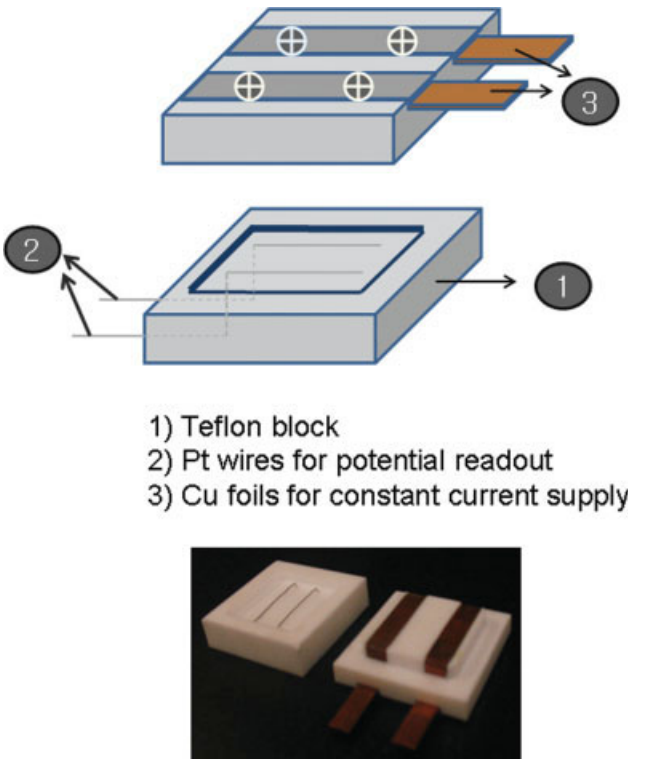


**Figure 1** Four-point-probe conductivity cell for measuring ionic conductivity in liquid and gel polymer electrolytes. [Color figure can be viewed in the online issue, which is available at www.interscience.wiley.com.]

The ionic conductivity of polymer electrolytes was measured at room temperature using lab-made four-probe conductivity cell, as shown in Figure 1.[12,28] The impedance of samples was determined using AC impedance analyzer (IM6e, ZAHNER, Germany). The impedance analyzer was worked in galvanostatic mode with AC current amplitude of 0.1 mA over frequency range form 1 MHz to 1 Hz by Nyquist method. The ionic conductivity was obtained as follows:

$$\sigma = \frac{L}{RS} \tag{1}$$

where σ is the ionic conductivity (in S/cm) and $L$ is the distance between the electrodes used to measure the potential (cm). $R$ is the impedance of the electrolyte (in Ω) and $S$ is the surface area for ion to penetrate the electrolyte (in $cm^2$). The impedance of each sample was measured three times to ensure data reproducibility.

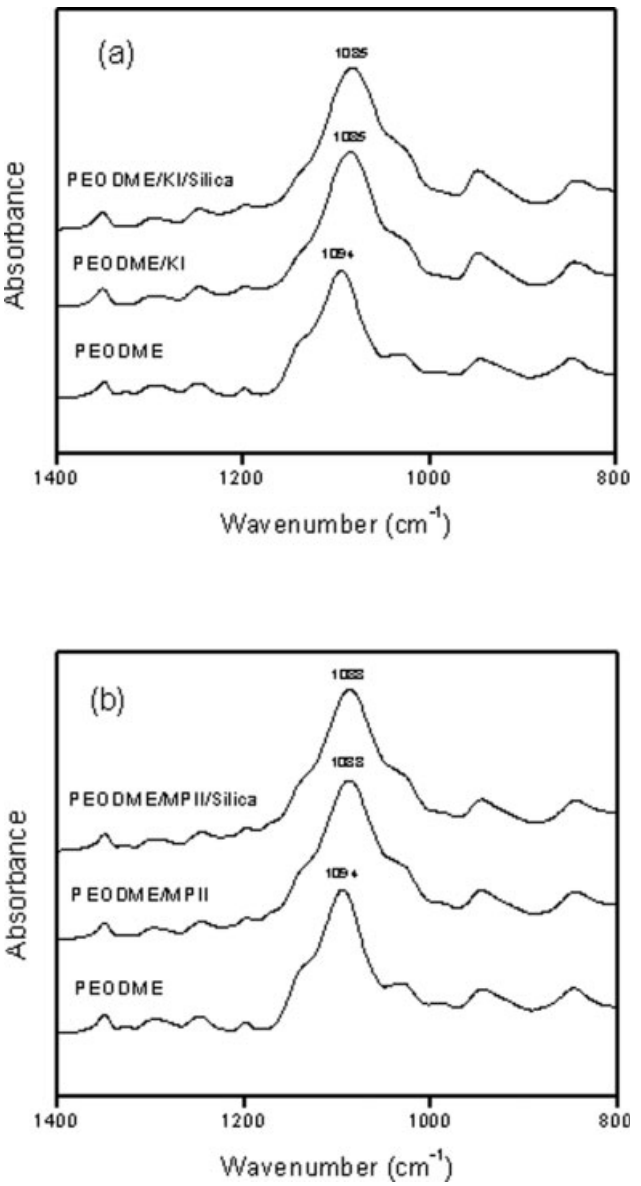


**Figure 2** FTIR spectra of neat PEODME, PEODME/MI, and PEODME/MI/silica nanoparticles electrolytes with 9 wt % of silica, where (a) M = $K^+$ and (b) M = imidazolium$^+$.

## RESULTS AND DISCUSSION

### Coordinative interactions in polymer electrolytes

The terminal group of PEG is different from that of PEODME; the former has hydroxyl (—OH) end group, whereas the latter has methyl ($—CH_3$) end group. Thus, the coordination site of two polymers to cations such as $K^+$ or imidazolium$^+$ might be different with each other. It is expected that PEODME interacts with cation mostly through ether oxygens. On the other hand, PEG contains two coordination sites of hydroxyl as well as ether oxygens, and thus competitive interaction is expected. However, PEG may preferentially interact with cations via hydroxyl group because the electron density of hydroxyl oxygen is larger than that of ether oxygen.[29,30]

To investigate the coordinative interaction between cations and ether oxygens of PEODME, the FTIR spectra of PEODME/MI (M = $K^+$ or imidazolium$^+$) electrolytes with and without fumed silica nanoparticles were measured. The mole ratio of ether oxygen to iodine salt was fixed at 20, and fumed silica nanoparticles was 9 wt % of total composite polymer electrolyte. The resultant spectra are presented in Figure 2. The free ether stretching band of pristine PEODME appeared at 1094 $cm^{-1}$. Upon the addition of salt in PEODME, the ether stretching band shifted to a lower wavenumber of 1085 and 1088 $cm^{-1}$ for KI and MPII, respectively. The shift to a lower wavenumber may be originated from the loosening of the C—O—C bond by the electron donation to cation.[31–33] The larger peak shift of KI electrolyte relative to MPII electrolyte reveals the stronger interaction of PEODME with KI than that with MPII. It was also found that the presence of fumed silica nanoparticles was not significantly involved in the coordinative interaction of the PEODME electrolytes, demonstrating that the solidification of polymer electrolytes resulting from the network formation of silica nanoparticles and the coordinative interactions are decoupled in the current experimental conditions, i.e., room temperature.

The FTIR spectra for neat PEG, PEG/KI, PEG/silica nanoparticles, and PEG/KI/silica nanoparticles electrolytes are presented in Figure 3. Neat PEG showed a broad absorption band, in which a maximum is positioned at 3375 $cm^{-1}$, attributable to the self-hydrogen bonded —OH stretching of PEG.[34,35] Free —OH band usually appears at around 3600

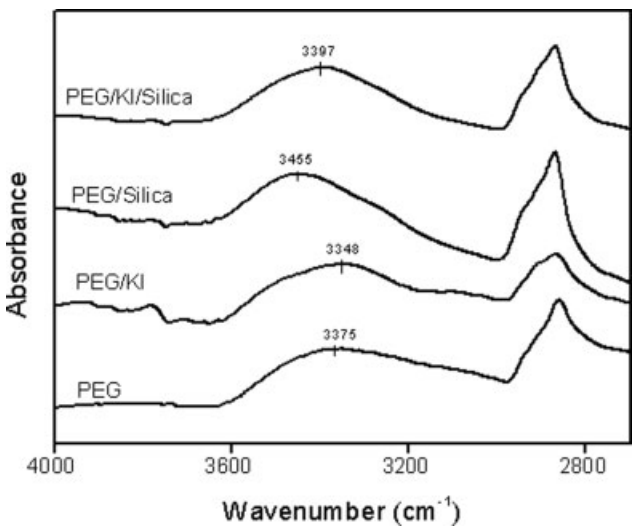


**Figure 3** FTIR spectra of neat PEG, PEG/KI, PEG/silica nanoparticles, and PEG/KI/silica nanoparticles electrolytes with 9 wt % of silica.

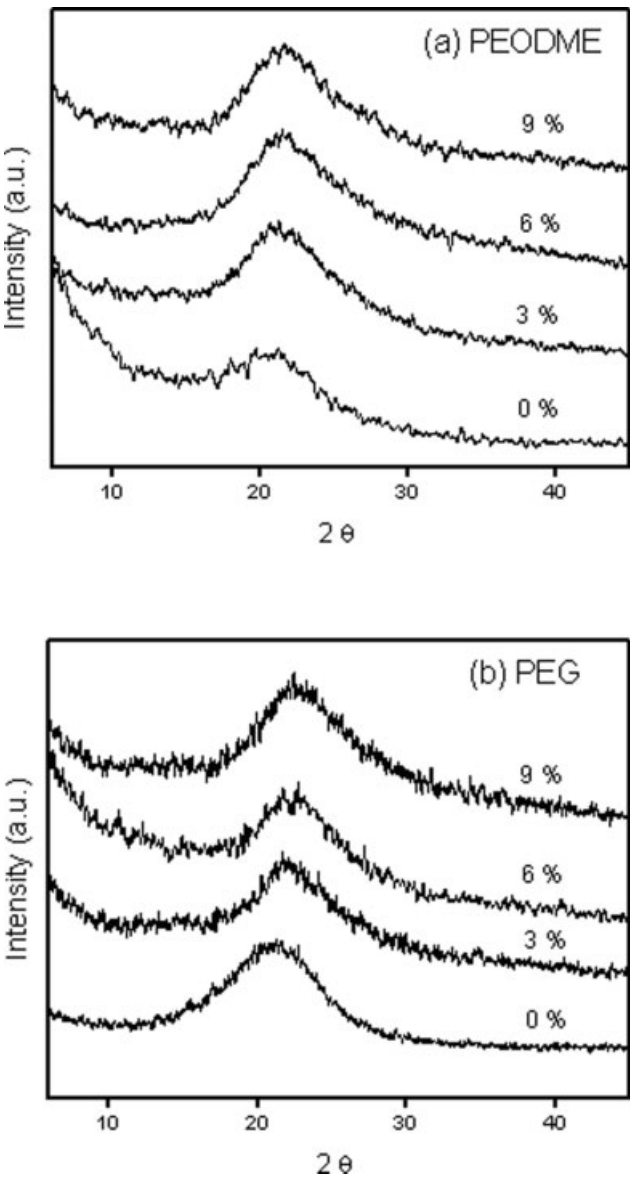


**Figure 4** WAXS spectra of polymer/KI/silica nanoparticles electrolytes with different concentration of silica where (a) PEODME and (b) PEG.

$cm^{-1}$.[35] The incorporation of KI in PEG led to the band shift toward a lower wavenumber at 3348 $cm^{-1}$, possibly due to the coordination of hydroxyl oxygen to potassium cation. In contrary, the introduction of fumed silica nanoparticles to PEG resulted in the band shift toward a higher wavernumber at 3455 $cm^{-1}$. This result represents that the relative interaction strengths between hydroxyl oxygen and other groups are arranged in the order.

$$\text{—OH}///\text{—SiOH} < \text{—OH}///\text{—OH} < \text{—OH}///K^+$$

In PEG/KI/silica nanoparticles electrolytes, the —OH group of PEG has three kinds of interaction site, i.e., $K^+$, —OH, and —SiOH. The maximum peak position at 3397 $cm^{-1}$ for PEG/KI/silica electrolyte lied between PEG/silica (—OH///—SiOH) and neat PEG (—OH///—OH), although the interaction of —OH///—SiOH is the weakest among them. This result represents the interaction between PEG and silica nanoparticles predominantly occurs in the PEG/KI/silica nanoparticles electrolytes.

### Structural change of polymer electrolytes

To investigate the structural change in polymer/MI (M = $K^+$, imidazolium$^+$)/silica nanoparticles electrolytes, WAXS spectra were measured. Figure 4 shows the WAXS results for two systems (PEODME and PEG), where broad amorphous hollows are shown, indicating the lack of crystalline part in both the pristine polymers and the polymer electrolytes. This represents that crystalline ionic salts are completely dissolved into amorphous-free ions in polymeric matrix due to coordinative interactions between the polymer and the cation of the salt. Thus, electrostatic interactions were considered negligible in the current system. Bragg *d*-spacing for the electrolytes was determined from the maximum position in the broad peak using Bragg relation. The values of Bragg *d*-spacing for two systems were plotted in Figure 5. As shown in this figure, Bragg *d*-spacing decreased with increasing concentration of fumed silica nanoparticles. It is presumably due to the chain contraction and/or densification in composite polymer electrolytes upon the addition of silica nanoparticles.[8] Especially, the *d*-spacings of PEG electrolytes exhibited lower values and sharper decline than those of PEODME electrolytes, implying more effective gelation formation in the former. This

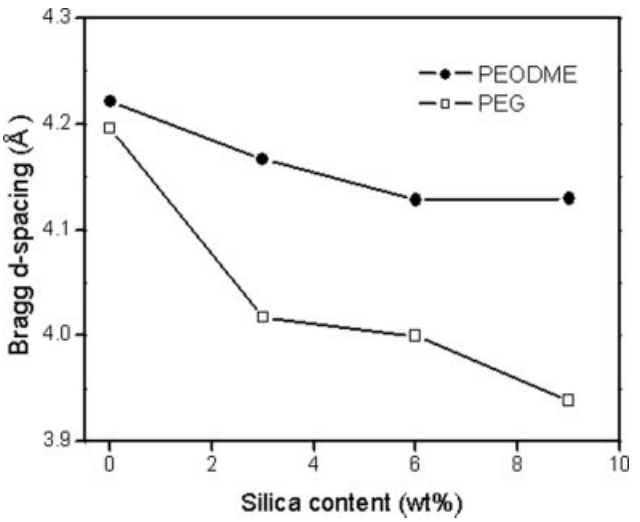


**Figure 5** Bragg *d*-spacing of polymer/KI/silica nanoparticles electrolytes as a function of silica content.

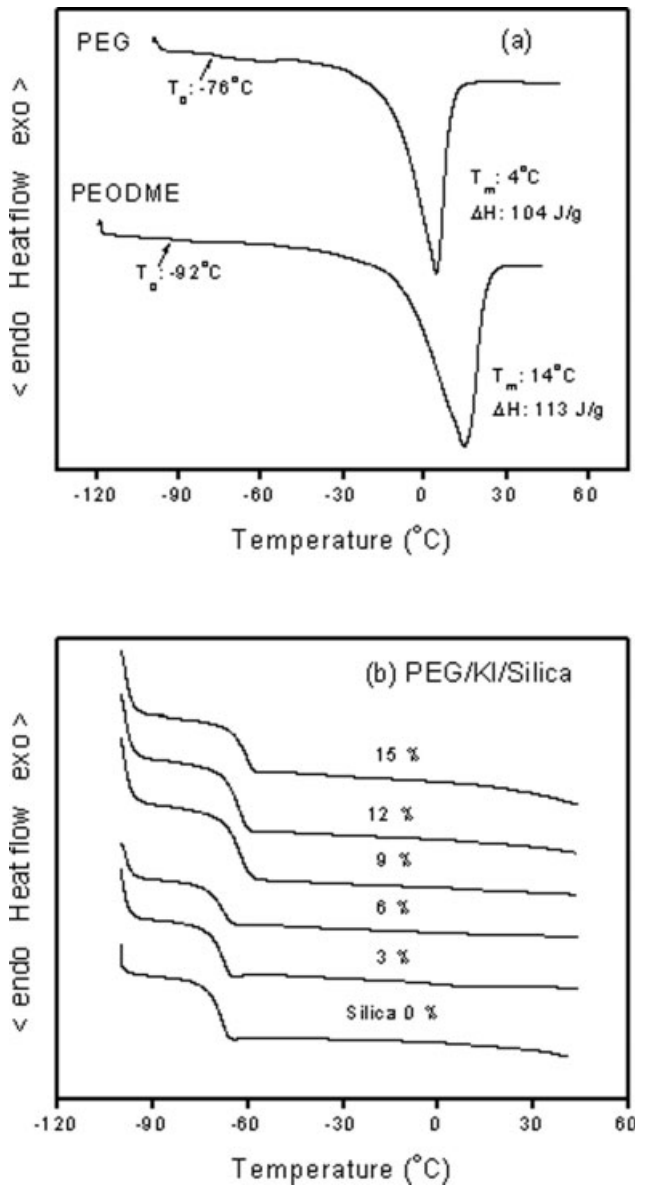


**Figure 6** DSC curves of (a) neat polymer (PEG, PEODME) and (b) PEG/KI/silica nanoparticles electrolytes as a function of silica content.

can be explained by the fact that PEODME interacts with cations mostly through ether oxygens whereas PEG does through the coordination sites of hydroxyl as well as ether oxygens, revealed by FTIR spectroscopy.

### Gelation of composite polymer electrolytes

The polymer electrolytes at low concentrations of silica nanoparticles are fluidic because the molecular weights of polymers used in this work are 400 and 500 g/mol for PEG and PEODME, respectively. With increasing amounts of silica nanoparticles, the polymer electrolytes lose their fluidity. The silica concentration at which the electrolyte becomes completely nonfluidic that is solidified was taken as a gelation point.

The DSC curves for the neat polymers and the composite polymer electrolytes were obtained. Neat PEG showed $T_g$ of $-76^\circ$C and $T_m$ of 4°C, whereas PEODME did $T_g$ of $-92^\circ$C and $T_m$ of 14°C, as shown in Figure 6(a). Thus, these two polymers are completely amorphous and liquid state at room temperature. The introduction of KI in the polymers led to the increase of $T_g$ (from $-76$ to $-70^\circ$C for PEG whereas from $-92$ to $-76^\circ$C for PEODME) and disappearance of $T_m$, as seen in Figure 6(b). The increase in $T_g$ is presumably due to the restriction of the chain mobility resulting from transient crosslinks between polymeric chains by metal coordination.[14,15] In the meanwhile, the decrease of crystallinity may be attributed to the fact that KI is dissolved to disrupt chain folding for crystallinity of polymer. The $T_g$ variation of the composite polymer electrolytes with different concentrations of fumed silica nanoparticles was compared in Figure 7 for two systems. The increase of silica content produced slight increase of $T_g$ up to 6 wt %, and abrupt jump-up at 9 wt %. It should be noted that 9 wt % is consistent with the threshold concentration in which the composite polymer electrolytes start to become solidified. Especially, the increase of $T_g$ in PEG system is higher than that in PEODME system, representing that the chain mobility is much hindered in the former system presumably due to the effective gelation formation. This result may be due to the fact that the hydroxyl groups of PEG participate in the gelation of the composite polymer electrolytes, consistent with WAXS result and verified by FTIR spectroscopy.

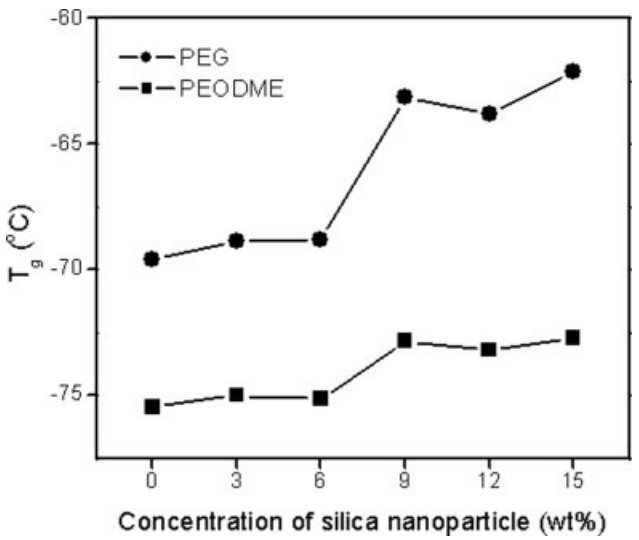


**Figure 7** $T_g$ variations of polymer/KI/silica nanoparticles electrolytes as a function of silica content.

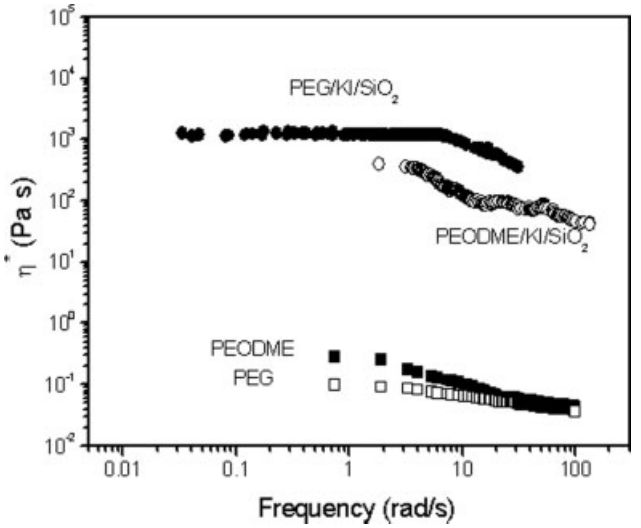


**Figure 8** Complex melt viscosities of pristine PEG, PEODME, and composite polymer electrolytes containing fumed silica nanoparticles of 9 w %.

A dramatic change in the viscosity of polymer electrolyte was characterized quantitatively using rheometer. The complex melt viscosities of pristine PEG, PEODME, and composite polymer electrolytes containing KI and fumed silica nanoparticles are presented in Figure 8 as a function of frequency. The concentration of fumed silica nanoparticles was fixed as 9 wt %. The zero shear viscosities of pristine PEG and PEODME at room temperature were as low as 0.1 and 0.25 Pa s, respectively. Slightly higher zero shear viscosity of the former may be related to the lower molecular weight of the former (400 g/mol) than the latter (500 g/mol). Upon the addition of KI and fumed silica nanoparticles, the zero shear viscosities of the electrolytes significantly increased to 1170 and 422 Pa s for PEG and PEODME, respectively. This result is directly indicative of the loss of fluidity of polymer electrolytes due to gelation phenomena by silica nanoparticles. It should also be noted that the viscosity of PEG electrolytes is higher than that of PEODME electrolyte, demonstrating more effective gelation formation of PEG electrolytes than PEODME electrolytes.

Schematic illustrations of gelation formation in the composite polymer electrolytes with increasing amounts of fumed silica nanoparticles were compared in Figure 9 for two electrolyte systems of PEG and PEODME. Polymer electrolytes without silica nanoparticles may have relatively weaker interactions in both systems. At intermediate concentrations of silica nanoparticles, silica nanoparticles may start to interact with the hydroxyl groups of PEG but not with the ether oxygens of ethylene oxides. This interpretation is supported by the FTIR spectroscopic results, as shown in Figures 2 and 3. At higher concentrations of silica nanoparticles, the hydrogen-bonding interaction between silica nanoparticles predominantly occurs, leading to the gelation formation of polymer electrolytes. Because of the participation of —OH groups of PEG in hydrogen-bonding interaction of silica nanoparticles, the gelation formation of PEG electrolytes becomes more effective than PEODME electrolytes, as revealed by WAXS, DSC, and viscosity results.

### Ionic conductivity of polymer electrolytes

The ionic conductivities of the composite polymer electrolytes, i.e., polymer (PEODME, PEG)/MI (M = $K^+$, imidazolium$^+$)/silica nanoparticles are presented in Figure 10 as a function of silica concentration. The ionic conductivities were measured at room temperature using a galvanostatic four-probe method. The ionic conductivity determined by four-probe method is higher to some degree but more accurate than that by two-probe method, due to the minimization of contact impedance.[36,37] The general behavior is that the ionic conductivities increase with the concentration of the fumed silica nanoparticles, reach a maxima at a silica concentration of around 9 wt %, and then decrease at higher silica concentrations. In terms of acid-base approach to

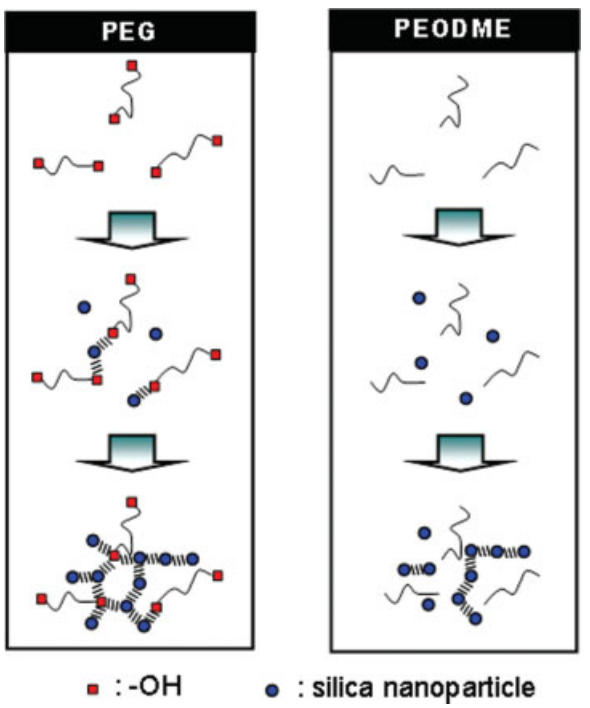


**Figure 9** Schematic illustration of gelation in composite polymer electrolytes with increasing amounts of fumed silica nanoparticles: (a) PEG and (b) PEODME. [Color figure can be viewed in the online issue, which is available at www.interscience.wiley.com.]

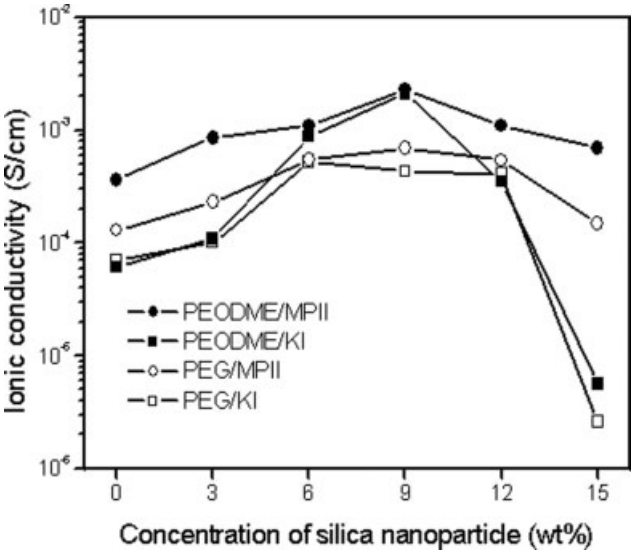


**Figure 10** Ionic conductivities of composite polymer electrolytes containing fumed silica nanoparticles as a function of silica content.

interaction mechanism, fumed silica nanoparticles ($SiO_2$) are considered as a weak Lewis acid.[25,38] Thus, fumed silica nanoparticles are expected to interact with iodine anion of the salt, which produces the weakened interaction between cation and anion. The reduced interaction between cation and counteranion increases the concentration of free ions in the polymer electrolytes, resulting in the increase of ionic conductivity. These interpretations are consistent with the previous reports.[23–25] On the other hand, the decrease of ionic conductivity above a certain composition is attributable to the strong solidification of polymer electrolytes by three-dimensional network formation with silica nanoparticles.[12]

The ionic conductivities of PEG-based electrolytes were lower than those of PEGDME electrolytes in all concentrations of silica nanoparticles when the same salt is used. It may be due to the more effective gelation formation of PEG electrolytes compared to PEODME electrolytes, as revealed by WAXS, DSC, and viscosity results. In addition, the composite polymer electrolytes containing MPII always exhibited higher ionic conductivities than those containing KI, implying that the ionic liquid is more effective than the metal salt in making the polymer chains flexible. It should also be noted that the maximum ionic conductivity of the composite electrolytes containing fumed silica nanoparticles is as high as $\sim 10^{-3}$ S/cm at room temperature.

## CONCLUSIONS

Nanocomposite polymer electrolytes consisting of low molecular weight PEO, MI (M = $K^+$, imidazolium$^+$) and fumed silica nanoparticles have been prepared and their thermal, structural, and coordination properties were investigated. The gelation of polymer electrolytes by fumed silica nanoparticles was strongly dependent on the end group of polymer matrix. The hydroxyl groups in PEG electrolytes took part in the hydrogen-bonding interaction between fumed silica nanoparticles, resulting in effective gelation formation compared to PEODME electrolytes, as revealed by WAXS, DSC, and viscosity measurement. Thus, the ionic conductivities of PEG electrolytes were always lower than those of PEODME electrolytes.

## References

1. Higa, M.; Fujino, Y.; Koumoto, T.; Kitani, R.; Egashira, S. Electrochim Acta 2005, 50, 3832.
2. Wang, X. L.; Mei, A.; Li, M.; Lin, Y.; Nan, C. W. Solid State Ionics 2006, 177, 1287.
3. Sata, T.; Kawamura, K.; Higa, M.; Matsusaki, K. J Membr Sci 2001, 183, 201.
4. Yamakawa, T.; Ishida, S.; Higa, M. J Membr Sci 2005, 250, 61.
5. Kang, M. S.; Kim, J. H.; Won, J.; Moon, S. H.; Kang, Y. S. J Membr Sci 2005, 247, 127.
6. Langsdorf, B. L.; Sultan, J.; Pickup, P. G. J Phys Chem 2003, 107, 8412.
7. Higa, M.; Yamakawa, T. J Phys Chem 2004, 108, 16703.
8. Kim, J. H.; Min, B. R.; Kim, C. K.; Won J.; Kang, Y. S. Macromolecules 2002, 35, 5250.
9. Olivetti, E. A.; Kim, J. H.; Sadoway, D. R.; Asatekin, A.; Mayes, A. M. Chem Mater 2006, 18, 2828.
10. Mui, S. C.; Jasinski, J.; Leppert, V. J.; Mitome, M.; Sadoway, D. R.; Mayes, A. M. J. Electrochem Soc 2006, 153, 1372.
11. Kim, Y. J.; Kim, J. H.; Kang, M. S.; Lee, M. J.; Won, J.; Lee, J. C.; Kang, Y. S. Adv Mater 2004, 16, 1753.
12. Kim, J. H.; Kang, M. S.; Kim, Y. J.; Won, J.; Park, N. G.; Kang, Y. S. Chem Commun 2004, 1662.
13. Stergiopoulos, T.; Arabatzis, I. M.; Katsaros, G.; Falaras, P. Nano Letters 2002, 2, 1259.
14. Kim, J. H.; Min, B. R.; Kim, C. K.; Won, J.; Kang, Y. S. J Phys Chem 2002, 106, 2786.
15. Kim, J. H.; Min, B. R.; Won, J.; Kang, Y. S. Macromolecules 2003, 36, 4577.
16. Fan, L.; Nan, C. W.; Zhao, S. Solid State Ionics 2003, 164, 81.
17. Fan, L.; Dang, Z.; Wei, G.; Nan C. W.; Li, M. Mater Sci Eng 2003, 99, 340.
18. Nan, C. W.; Fan, L. Z.; Lin, Y. H.; Cai, Q. Phys Rev Lett 2003, 91, 266104.
19. Croce, F.; Curini, R.; Martinelli, A.; Persi, L.; Ronci, F.; Scrosati, B.; Caminiti, R. J Phys Chem 1999, 103, 10632.
20. Su, S. J.; Kuramoto, N. Synth Met 2000, 114, 147.
21. Ray, S. S.; Biswas, M. Synth Met 2000, 108, 231.
22. Cheung, I. W.; Chin, K. B.; Greene, E. R.; Smart, M. C.; Abbrent, S.; Greenbaum, S. G.; Prakash, G. K. S.; Surampudi, S. Electrochim Acta 2003, 48, 2149.
23. Xiong, H. M.; Zhao, K.-K.; Zhao, X.; Wang, Y. W.; Chen, J. S. Solid State Ionics 2003, 159, 89.
24. Chung, S. H.; Wang, Y.; Persi, L.; Croce, F.; Greenbaum, S. G.; Scrosati, B.; Plichta, E. J. Power Sources 2001, 97, 644.
25. Swierczynski, D.; Zalewska, A.; Wieczorek, W. Chem Mater 2001, 13, 1560.
26. Raghavan, S. R.; Riley, M. W.; Fedkiw, P. S.; Khan, S. A. Chem Mater 1998, 10, 244.

27. Hou, J.; Baker, G. L. Chem Mater 1998, 10, 3311.
28. Kang, M.-S.; Kim, J. H.; Won, J.; Kang, Y. S. J Photochem Photobio Part A: Chem 2006, 183, 15.
29. Kim, J. H.; Min, B. R.; Lee, K. B.; Won, J.; Kang, Y. S. Chem Commun 2002, 2732.
30. Kim, J. H.; Min, B. R.; Won, J.; Kim, C. K.; Kang, Y. S. J Polym Sci Part B: Polym Phys 2004, 42, 621.
31. Hong, L.; Cui, Y.; Wang, X.; Tang, X. J Polym Sci Part B: Polym Phys 2003, 41, 120.
32. Basak, P.; Manorama, S. V. Eur Polym J 2004, 40, 1155.
33. Zalewska, A.; Stygar, J.; Ciszewska, E.; Wiktorko, M.; Wieczorek, W. J Phys Chem 2001, 105, 5847.
34. Vien, D. L.; Colthup, N. B.; Fateley, W. G.; Grasselli, J. G. The Handbook of Infrared and Raman Characteristic Frequencies of Organic Molecules; Academic Press: Boston, 1991.
35. Noto, V. D.; Longo, D.; Munchow, V. J Phys Chem 1999, 103, 2636.
36. Cahan, B. D.; Wainright, J. S. J Electrochem Soc 1993, 140, L185.
37. Lee, C. H.; Park, H. B.; Lee, Y. M.; Lee, R. D. Ind Eng Chem Res 2005, 44, 7617.
38. Wieczorek, W.; Lipka, P.; Zukowska, G.; Wyciślik, H. J Phys Chem B 1998, 102, 6968.